8. D. B. Ericson, M. Ewing, G. Wollin, B. C. Heezen, *Bull. Geol. Soc. Amer.* **72**, 193 (1961).
9. ———, *Science* **146**, 723 (1964).
10. F. B. Phleger, F. L. Parker, J. F. Peirson, *Rep. Swedish Deep Sea Exp. (1947-1948)* **7**, 1 (1953).
11. F. L. Parker, *ibid.* **8**, No. 4, 219 (1958).
12. R. Todd, *ibid.* **8**, No. 3, 169 (1958).
13. Five-percent error on species distribution is achieved by using an average of 710 specimens per sample and verified by the use of Tchebycheff's theorem [H. Cramer, *The Elements of Probability Theory* (Wiley, New York, 1955), p. 81].
14. A. R. Loeblich, Jr., *et al., U.S. Nat. Mus. Bull. 215* (1957).
15. W. Kemp and D. Eger, *J. Geophys. Res.*, in press. Error measure is the optimum measure in percentage of the amount of correlation between two time series with random components.
16. J. I. Jones, data presented at International Co-operative Investigations of the Tropical Atlantic Symposium, Abidjan, October 1966.
17. J. S. Bradshaw, *Contrib. Cushman Found. Foraminiferal Res.* **10**, 25 (1959).
18. ———, *J. Paleontol.* **31**, 1138 (1957).
19. N. Watabe and K. M. Wilber, *Limnol. Oceanogr.* **11**, 567 (1966).
20. R. E. Arnal, *The Compass* (Sigma Gamma Epsilon Soc.) **32**, 185 (1955).
21. L. Lidz, *Limnol. Oceanogr.* **10**, 392 (1965).
22. J. G. Watkins, *Micropaleontology* **5**, 101 (1959).
23. J. I. Jones, *Bull. Amer. Ass. Petrol. Geol.* **50**, 619 (1966).
24. A. W. H. Bé, *Micropaleontology* **6**, 373 (1960).
25. A. B. Smith, *Contrib. Cushman Found. Foraminiferal Res.* **14**, 1 (1963).
26. R. Casey, *Bull. Amer. Ass. Petrol. Geol.* **47**, 1768 (1963).
27. B. J. Enbysk, *ibid.* **49**, 1760 (1965).
28. L. Lidz, *Limnol. Oceanogr.* **11**, 257 (1966).
29. I thank Barbara Lidz for illustrations of foraminifera, W. Kemp for providing the computer program so that all data in this report could be processed by an I.B.M. 7040 computer, and C. Emiliani for his continued encouragement. Financial support provided by NSF grant GP-5012.
30. Contribution No. 715 from the Institute of Marine Science, University of Miami.

10 October 1966

Inverse Compton Effect: Some Consequences for Quasars

Abstract. *The inverse Compton effect can transform enough energy of relativistic electrons into radiation so that an upper limit to the mean energy of the electrons is set. In quasars, the limit is too small to allow the production of any appreciable amount of synchrotron or inverse Compton radiation, unless either the distances are not cosmological or the lifetimes of the relativistic electrons are extremely short, of the order of hours.*

The inverse Compton effect increases the energy of photons by collisions of the photons with high-energy electrons. If the energy transfer caused by each collision is too large, then the radiation density and accordingly the Compton losses will grow continuously. This growth is stopped by the breakdown of the energy stored in the relativistic electrons. Thus the mean energy of the electrons is reduced below a critical value; the characteristic time is $< R/c$ (R, radius of the quasar). This holds even when energy is continuously resupplied. Therefore, the inverse Compton effect limits the possible mean energy of the relativistic electrons and thus puts restrictions on quasar models.

By E_e (in metric units) and γ_e (in units of the rest energy m_0c^2 of the electrons) we denote the energy of individual relativistic electrons, while E and γ (without subscript) are the mean values averaged over all relativistic electrons.

The total radiation power of an electron of energy $E_e = m_0c^2\gamma_e$ as it is scattered by low-energy photons of radiation density U is (*1*)

$$p_e = 4\,c\,\sigma_0\,\gamma^2\,U/3 \qquad (1)$$

where $\sigma_0 = 6{\cdot}10^{-25}$ cm^2, which is the Thompson cross section. If U contains photons of frequencies up to the ultraviolet, the formula is valid for $30 < \gamma_e < 10^4$ and may be used for approximations also with higher values of γ_e. If we replace the mean radiation power $P_c \equiv p_c\ (\gamma)$ by the corresponding Compton luminosity $L_c = 4\pi R^3 N_e P_c/3$ (which is possible only if L_c is approximately constant within a time of the order of R/c), then

$$L_c = 4\,R\sigma_0\,N_e\,\gamma^2\,L/3 \qquad (2)$$

N_e is the number density of relativistic electrons, and $L = 4\pi R^2\ c\ U/3$, the total luminosity. If we write $L = L_t + L_s + L_c$ (L_t denoting a possible thermal component, L_s the synchrotron component), it is obvious from Eq. 2 that the inequality

$$4\,R\sigma_0\,N_e\,\gamma^2/3 \leqq (L_c + L_s)/L \leqq 1 \qquad (3)$$

must hold. As long as the left-hand side is > 0.5, the inverse Compton effect, as compared to the synchrotron mechanism and any thermal emission, is dominating.

The mean lifetime of the relativistic electrons, defined as the time in which half of the energy is lost by radiation, is $\tau = E/P$, where $E = m_0\,c^2\,\gamma$ is the mean electron energy, and $P = P_c + P_s$. Here, P_s denotes the mean radiation power due to synchrotron emission.

From Eq. 3 it follows that

$$\gamma \leqq \frac{3(L_c + L_s)}{4\,R\sigma_0\,N_e\,\gamma\,L} = \frac{3}{4\,R\sigma_0\,L\,N_e} \times \frac{4\ \pi R^3\ N_e\ (P_c + P_s)}{3} \cdot \frac{m_0\,c^3}{\tau\ P} = \frac{\pi\,R\,m_0\,c^3}{\sigma_0\,L} \cdot \frac{R}{c\ \tau}$$

L cannot be measured directly but has to be calculated from the observed intensity by means of an assumed photometric distance, D_a. If D is the real photometric distance, the actual luminosity differs from the calculated one by a factor $(D/D_a)^2$.

With typical values for quasars: $R = 10^{17}$ cm, $L = 3{\cdot}10^{46}$ erg per second (luminosity calculated from a cosmological interpretation of the red shifts)

$$\gamma \leqq 0.5\ (D/D_a)^{-2}\ (\tau c/R)^{-1} \qquad (5)$$

On the other hand, the fact that nonthermal radiation is emitted by quasars gives a lower limit for γ. In order that any appreciable amount of synchrotron or inverse Compton radiation be emitted at all, it is necessary that $\gamma > 30$. Furthermore, in order that energy be emitted in a frequency range of several orders of magnitude it is probable that γ has a still higher value, at least of the order of 10^2. It is impossible to give a definite estimate of γ without using more detailed characteristics of the radiation spectrum. In any case, the upper limit of γ given by Eq. 5 must exceed the lower limit, and therefore at least one of the factors in Eq. 5 should be appreciably larger than unity. In other words, in a "cosmological" quasar model with large electron lifetimes the mean electron energy would be limited by Eq. 5 to an impossibly small value. This conclusion is independent from whether or not the major part of the radiation is due to the inverse Compton effect. So we are left with two possibilities.

The first is that the assumed distances are too large. Terrell's hypothesis (*2*), of a gigantic explosion in the Milky Way some 10^7 years ago reduces the distance by a factor of about 10^3. By use of this factor in Eq. 5, it follows that the mean lifetime of the relativistic electrons may be appreciably larger than R/c, but should not exceed a few hundred years.

Under the second possibility we assume that the cosmological interpretation of the red shifts is correct. Then it follows that the lifetime of the relativistic electrons must be extremely short, of the order of minutes to hours.

In this case, the relativistic electrons are created *in situ*, that is, at any place within the quasar where the radiation is generated. This makes it likely that the relativistic electrons (and positrons) are secondary products of high-energy protons. The total energy output is now solely determined by the creation rate of the relativistic electrons and positrons. A magnetic or radiation field, or both, may only influence the spectral distribution of the radiation.

These two alternatives were also obtained by Hoyle, Burbidge and Sargent (*3*), who used the observed spectral characteristics of the quasar radiation in their analysis.

The lifetime τ_e of individual electrons is proportional to $1/\gamma_e$ and is connected with the mean values τ and γ by

$$\tau_e = \gamma\tau/\gamma_e \qquad (6)$$

If we combine this equation with Eq. 5 then it follows that within the cosmological hypothesis the individual lifetimes are smaller than R/c for all electrons whose energy is high enough to contribute to the nonthermal radiation ($\gamma_e > 30$). The reason is that the actual lifetime must be still smaller than the lifetime due to Compton radiation alone, which itself is smaller than R/c for all sufficiently large values of γ_e.

J. PFLEIDERER
M. GREWING
Astronomische Institute der Universität, Bonn, Germany

References and Notes

1. J. E. Felten and P. Morrison, *Phys. Rev. Letters* **10**, 453 (1963).
2. J. Terrell, *Science* **145**, 918 (1964); J. H. Hunter, S. Sofia, E. Fletcher, *Nature* **210**, 346 (1966).
3. F. Hoyle, G. R. Burbidge, W. H. L. Sargent, *ibid.* **209**, 751 (1966).
4. We thank Dr. W. Priester for discussion. Mitteilungen der Astronomischen Institute der Universität Bonn, No 74.

16 August 1966

Crystal Structure of Kernite, $Na_2B_4O_6(OH)_2 \cdot 3H_2O$

Abstract. *Kernite, $Na_2B_4O_6(OH)_2 \cdot 3H_2O$, contains parallel infinite chains of the borate polyanion $[B_4O_6(OH)_2]_n^{2n-}$. The chains are composed of six-membered rings containing one boron-oxygen triangle and two boron-oxygen tetrahedra. The rings are linked through commonly shared boron-oxygen tetrahedra.*

The mineral kernite is a member of the borate group $Na_2O \cdot 2B_2O_3 \cdot nH_2O$ where $n = 0$, 1, 2, 4, 5, and 10. Of this group, only the structure of the decahydrate (borax) is known (*1*). The borax polyanion consists of two boron-oxygen triangles and two boron-oxygen tetrahedra which share corner oxygens. By analogy to other hydrated borate systems, it was thought that the lower hydrates would be formed by polymerization of the borax anion into chains or other three-dimensional arrangements, with the removal of H_2O (*2*). In addition, Christ and Garrels (*3*) suggested that in kernite the borax polyanion had itself been altered. The structure of kernite ($n = 4$) has now been solved, and the result substantiates these ideas.

The structure was solved with the use of approximately 1800 x-ray diffraction intensities. A General Electric XRD-6, equipped with a scintillation counter and CuKα radiation monochromatized by a balanced pair of Ni and Co filters, was used for these measurements. The symbolic-addition method of Karle and Karle (*4*) yielded directly the phases of 225 of the largest normalized structure factors. I computed a three-dimensional Fourier map using the phases so determined and the normalized structure factors which revealed 14 of the 17 nonhydrogen atoms in the asymmetric unit. Refinement proceeded with least-squares techniques and a difference electron-density map for the location of the three missing atoms. The present residual factor is 0.10 for all reflections. The relevant crystallographic data for kernite and a list of atomic coordinates at the present stage of refinement are shown in Table 1. An anisotropic temperature-factor refinement is in preparation.

The average distances between B and O in the polyanion are 1.37 Å in the triangles and 1.48 Å in the tetrahedra. The Na^+ ions are surrounded by six oxygens in an irregular manner. The Na^+-coordination polyhedra share some edges and corners to form a three-dimensional network around the anions. The average Na—O distance is 2.41 Å.

The borate polyanion in kernite consists of six-membered boron-oxygen rings which share tetrahedral boron atoms. These form infinite chains which extend in the *b* direction, two in each unit cell. Because of the manner in which the rings share boron atoms the plane of each successive ring is approximately 90° to the plane of the preceding ring. Since the shared boron atoms are adjacent in each ring, the chain forms a spiral in the direction of the *b*-axis. From a projection of the polyanion viewed down the *a*-axis (Fig. 1) all the oxygen atoms take part in bonding between boron atoms, except for the

Table 1. Atomic coordinates for kernite $Na_2B_4O_6(OH)_2 \cdot 3H_2O$. Monoclinic $P2_1/c$: $a = 7.0172 \pm 0.0006$; $b = 9.1582 \pm 0.0006$; $c = 15.6774 \pm .0015$ Å; $\beta = 108.861° \pm .002°$; cell volume = 953.4 Å^3; $z = 4$; density = 1.93 (calc.), [(obs.) 1.91 g cm^{-3}].

Atom	Coordinates (in fractions of cell edges)		
	x	*y*	*z*
Na_1	0.319	0.465	0.311
Na_2	.186	.367	.072
O_1	.511	.025	.397
O_2	.440	.099	.241
O_3	.768	.205	.269
O_4	.465	.351	.209
O_5	.792	.448	.215
O_6 (OH)	.064	.290	.240
O_7 (OH)	.585	.295	.011
O_8 (H_2O)	.774	.034	.067
O_9	.565	.272	.362
O_{10} (H_2O)	.037	.062	.414
O_{11} (H_2O)	.167	.117	.077
B_1	.552	.167	.421
B_2	.552	.232	.269
B_3	.572	.481	.200
B_4	.866	.315	.243

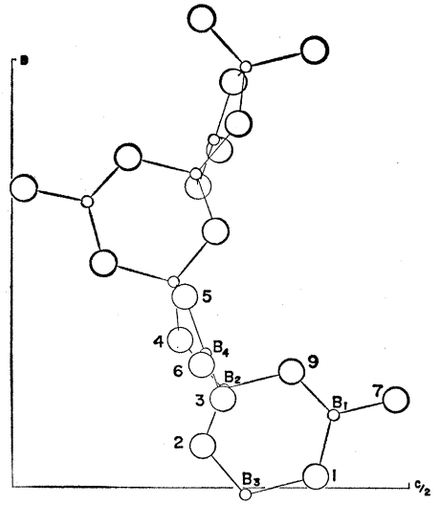

Fig. 1. Projections of the borate polyanion $[B_4O_6(OH)_2]_n^{2n-}$ viewed along the *a*-axis. The small circles are boron atoms; the large circles are oxygen atoms, except for the circles at Nos. 6 and 7 which are hydroxyl groups. The numbering conforms to Table 1.